Tunable high-purity microwave signal generation from a dual-frequency VECSEL at 852 nm (orale)

Fabiola A. Camargo, Nils Girard, Jean-Marie Danet, Ghaya Baili, Loïc Morvan, Daniel Dolfi, David Holleville, S. Guérandel, Isabelle Sagnes, Patrick Georges, et al.

Tunable high-purity microwave signal generation from a dual-frequency VECSEL at 852 nm

F. A. Camargo[1], N. Girard[2], J.M. Danet[3], G. Baili[2], L. Morvan[2], D. Dolfi[2], D. Holleville[3], S. Guerandel[3], I. Sagnes[4] , P. Georges[1], G. Lucas-Leclin[1]
[1]Laboratoire Charles Fabry, Institut d'Optique, CNRS, Univ Paris-Sud XI , Palaiseau, France
[2]Thales Research & Technology, Palaiseau, France
[3]LNE-SYRTE, Systèmes de Référence Temps-Espace, Observatoire de Paris, CNRS, UPMC , Paris, France
[4]Laboratoire de Photonique et de Nanostructures, CNRS, Marcoussis, France

ABSTRACT

We demonstrate the dual-frequency emission of a diode-pumped vertical external-cavity semiconductor laser operating at 852 nm, dedicated to the coherent population trapping of cesium atoms for compact atomic frequency references. It is based on a single laser cavity sustaining the oscillation of two adjacent, cross-polarized, modes. The output power reaches 10 mW on each frequency. The frequency difference and the absolute laser frequencies are simultaneously precisely tuned and stabilized on external references, resulting in the generation of a high-purity optically-carried microwave signal. The laser design has focused on stability and compactness.

Keywords: Vertical Cavity Surface-Emitting Lasers, Metrology

1. INTRODUCTION

Coherent population trapping (CPT) has been demonstrated as an interesting technique for compact atomic frequency references [1,2] and quantum information. It is based on the coupling of the two hyperfine ground states of an alkali atom through excitation to a common atomic level by two phase-coherent laser fields nearly resonant with the atomic transitions. With ^{133}Cs atoms, the hyperfine frequency splitting in the microwave range is equal to 9.192631770 Hz and is used for the second definition; the pair of laser fields has to be tuned either at the D1 (894 nm) or D2 (852 nm) optical transition line. When the phase-coherent laser fields are precisely resonant with the atomic transitions, Cs atoms are trapped in a "dark" state and stop interacting with the laser light: it corresponds to a narrow transmission line in the Cs absorption spectrum, which is used as a frequency reference.

The common solutions for the realization of the coherent pair of laser beams are sideband generation by microwave modulation of a single-frequency diode laser laser [1] (either directly through injection current or externally with an electro-optic modulator) and optical phase-locking of two independent lasers [2]. The latter configuration is ideal from a metrological point of view and it is commonly used nowadays in atomic clock experiments, however it requires a complex and costly wideband phase-locked electronics loop.

Meanwhile, the dual-frequency emission of a solid-state laser has been demonstrated, based on the simultaneous emission of two cross-polarized longitudinal modes inside the same laser cavity: a frequency difference in the GHz range has been obtained with a Nd:YAG laser crystal [3] and in the THz range with a Yb:KGW [4]. A similar configuration has been recently demonstrated with an optically-pumped vertical-external-cavity semiconductor laser (OP-VECSEL) operating at 1 μm [5]. In these cavities, an intracavity birefringent component induces a phase anisotropy which forces the laser to operate on two longitudinal modes, corresponding respectively to the ordinary and extraordinary polarization. As they share the same cavity, the two cross-polarized laser lines experience strongly correlated frequency and intensity fluctuations. The frequency difference may be tunable from few tens of MHz to a few THz by adjusting the intracavity phase anisotropy.

We investigate here the dual-frequency operation of an OP-VECSEL emitting at the D2 line of Cs atoms (λ = 852 nm), with a frequency difference tunable in the microwave range and optical properties compatible with the coherent

population trapping of Cs atoms. Dual-frequency operation of an OP-VECSEL presents indeed many advantages: first of all, the active structure can be designed for laser emission at the desired wavelength; emission at λ = 852 nm from AlGaAs-based devices has been obtained with output power in the Watt range [6]. Additionally, centimeter-long-cavity VECSEL do not present relaxation oscillations thanks to a class-A dynamical behavior, which results from a photon lifetime inside the laser cavity longer than the excited-carriers lifetime [10]. Thus the relative-intensity-noise (RIN) is low, shot-noise limited on a wide spectral range. Finally, high-power single-frequency operation of OP-VECSEL, with narrow spectral linewidth, has already been established [7][8].

2. DESIGN OF THE DUAL-FREQUENCY EMISSION LASER

2.1 Semiconductor structure

The 1/2-VCSEL chip has been grown by metal-organic chemical-vapor deposition on a 350 µm thick GaAs substrate and is designed for emission at λ_L = 852 nm under barrier-pumping at λ ≤ 700 nm. Since red laser sources are neither as efficient nor as powerful as in the infrared range, the active structure has been carefully designed to reach a low laser threshold while keeping the highest gain achievable [9]. The 30λ/4-thick active region is composed of seven 8-nm thick GaAs quantum wells, embedded between $Al_{0.22}Ga_{0.78}As$ barriers. The QW's are distributed among the optical standing-wave antinodes positions with a repartition 1-1-1-1-0-1-0-1-0-0-1 (from the top surface) which is calculated in order to provide a nearly constant excited carrier density among them. The active structure is resonant at the design wavelength, which increases its effective optical gain [11]. The bottom Distributed Bragg Reflector (DBR) consists of 32.5 pairs of $AlAs/Al_{0.225}Ga_{0.775}As$ λ/4-thick layers, and its reflectivity is evaluated to R > 99.95% at 852 nm. Finally, two 30-nm thick $Al_{0.39}Ga_{0.61}As$ layers produce a potential barrier at the Bragg mirror/active region interface and at the top surface for carrier confinement, and the structure has been protected by a 50-nm thick $In_{0.48}Ga_{0.52}P$ capping layer against oxidation of the Al-rich barrier layers.

As no anti-reflection coating is deposited on the top surface of the structure to ensure the resonant gain design, about 30% of the incident pump beam is reflected on the surface; the internal pump absorption in the barriers is evaluated to 90% in single-pass for wavelengths around 680 nm. Finally, it is noteworthy that the semiconductor chip is used as grown on its 350 µm-thick GaAs substrate.

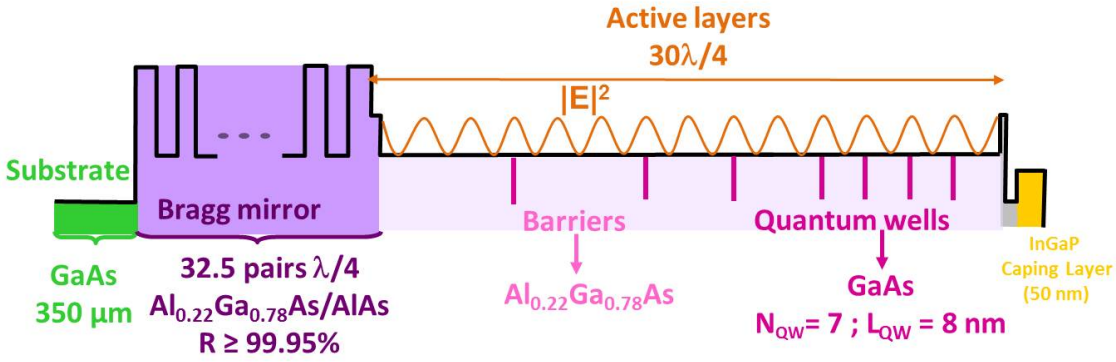

Figure 1: Semiconductor structure design.

2.2 Dual-frequency emission laser cavity

The pump source is a 1.6 W-broad-area laser diode emitting at 670 nm coupled into a 100 µm diameter, NA = 0.22, multimode fiber. This source delivers almost 1 W at the fiber end. The pump beam is focused on the semiconductor chip with two doublets of f_1 = 25 mm and f_2 = 19 mm under a 50° angle, yielding a 70 µm × 110 µm-elliptical spot on the structure. The laser cavity is composed by the semiconductor chip and a 15 mm concave output mirror with a transmission of 0.5% at 852 nm. The cavity length is 10 mm, resulting in a laser beam diameter of ~70 µm in the structure (Figure 2 right). A 50 µm –thick uncoated silica etalon is inserted in the cavity to ensure a single-frequency operation and to tune the laser wavelength at the Cs D2 line at 852.14 nm

The dual frequency emission is obtained by introducing a birefringent element in the laser cavity, which controls the phase anisotropy inside the cavity and results in the emission of two cross-polarized lines within the same laser cavity. We use a 500µm-thick antireflection coated YVO_4 plate cut at 45° to its optic axis, which induces a spatial separation of 50 µm between the extraordinary and ordinary beams in the structure in the longer axis of the pump ellipse (Figure 2 left). Indeed, the spatial separation of the two polarized beams reduces the nonlinear coupling between them and is thus necessary to ensure a stable dual frequency emission [12]. Eventually, the frequency difference Δν between the two polarizations is adjusted by an intracavity MgO:SLT electro-optic modulator (Figure 2 right), whose birefringence changes with both the temperature and the applied voltage. With all the elements inside the cavity, the FSR of the laser cavity is FSR_C = 12 GHz.

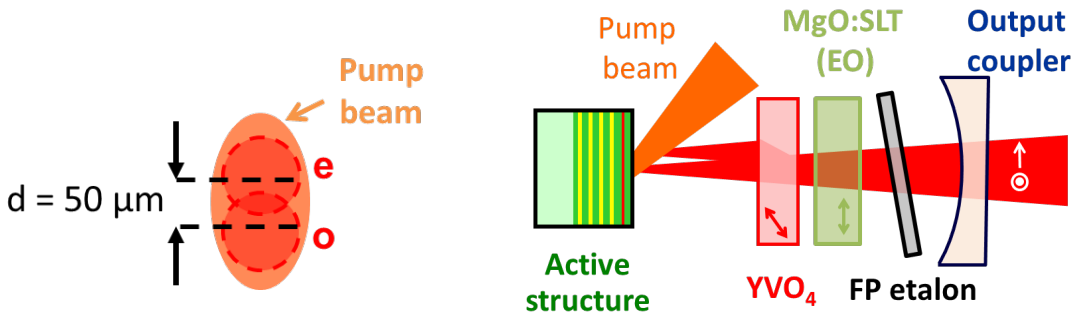

Figure 2: Experimental setup for the OP-VECSEL (right) and the laser and pump beam overlap on the chip surface (left).

The laser cavity design has focused on compactness as well as high mechanical and thermal stability. The pump optics, the semiconductor chip and the laser cavity elements are integrated in a compact 90 mm × 90 mm × 40 mm casing. This limits mechanical and acoustic vibrations as well as air temperature fluctuations inside the external cavity. The temperature of the whole setup is stabilized to 24°C. The semiconductor chip is fixed on a thermoelectric and its temperature is controlled at 16°C using a Peltier element. The output coupler is glued on a piezo-electric transducer (PZT) for the fine adjustment of the cavity length.

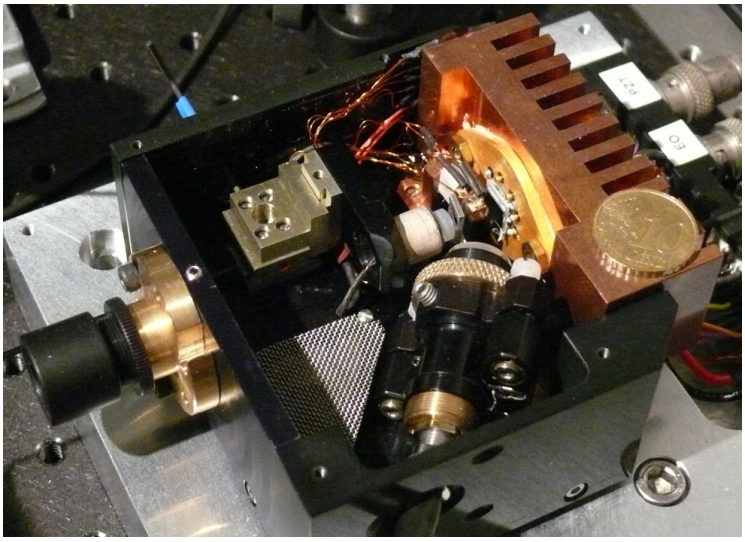

Figure 3 : Photo of the compact prototype designed for this project.

2.3 Frequency difference tunability

The birefringence introduced in the laser cavity results in slightly different optical paths for each polarization (respectively ordinary and extraordinary), which produce two combs of longitudinal modes distanced by Δν. The

frequency difference Δν is related to the intracavity phase anisotropy Δϕ and the FSR_C of the laser cavity through the relationship:

$$\Delta\nu = \nu_e - \nu_o = \frac{\Delta\phi}{\pi}\frac{c}{2L} \tag{1}$$

where c is the light velocity, L is the laser cavity length. The frequency difference Δν is finely tuned with the help of the electro-optic crystal inside the cavity. We use here a stoichiometric Lithium Tantalate (SLT) crystal with dimensions of 2×2×1 mm^3 (H×L×W); in order to avoid photorefractive effects this crystal is doped with 5% of MgO. The crystal birefringence changes with the applied voltage following the relationship:

$$\Delta\phi = \frac{2\pi}{\lambda}\frac{l}{e}V\left(\frac{n_e^3}{2}r_{33} - \frac{n_o^3}{2}r_{13}\right) \tag{2}$$

where λ is the laser wavelength, l is the crystal length, e is the distance between the two electrodes used to applied a voltage V in the crystal, n_e and n_o are the index refraction at the extraordinary and ordinary polarization, respectively and r_{33} and r_{13} are the electro-optic coefficient along the axes x and z, respectively, where x is the axis where the voltage is applied and z is along the beam propagation. Additionally, the crystal birefringence changes with the temperature – because of dilatation and refractive index change – following :

$$\frac{\partial\phi}{\partial T} = \frac{2\pi}{\lambda}\frac{\partial l}{\partial T}\left(n_e - n_{\grave{a}}\right) + \frac{2\pi}{\lambda}l\left(\frac{\partial n_e}{\partial T} - \frac{\partial n_o}{\partial T}\right) \tag{3}$$

Refractive index at 25°C	$n_e = 2.1418$ $n_o = 2.1441$
Electro-optic coefficient (pm/V)	$r_{13} = 6.96$ $r_{33} = 29.6$
Thermal expansion $\partial l/\partial T$ (K^{-1})	1.5×10^{-5}

Table 1: Parameters of the MgO: SLT crystal [13][14].

Assuming a cavity length 10mm, a crystal thickness e = 2 mm and a crystal length l = 1 mm, the frequency difference tunability as function of the voltage applied in the crystal is evaluated to 1.59 MHz/V. The frequency difference tunability with the temperature is calculated at 1.25 GHz/K at 852 nm; this value is large, and demonstrates that a coarse tunability of Δν will be achieved in order to obtain the desired value of Δν = 9.2 GHz. Experimentally, the tunability coefficients are measured to be 1.3 MHz/V and 1.4 GHz/K, in good agreement with the theoretical values.

3. LASER CHARACTERIZATION

First of all the laser is characterized without intracavity elements. The laser output power reaches 83 mW at 855 nm, in a multimode spectrum, and the laser threshold is 0.25 W incident pump power. Using a Fabry-Perot etalon with a free-spectral-range FSR_e = 2THz, the laser exhibits a single longitudinal mode emission, with a tunability of almost 5 nm. With the etalon, the YVO_4 plate and the MgO:SLT crystal inside the cavity, the laser output power decreases to 26 mW at 852.1 nm, corresponding to 13 mW per polarization (Figure 4). The laser threshold increases to 0.35 W. due to the additional optical losses introduced by the intracavity elements. The fine tunability of the laser lines is achieved with the rotation of the Fabry-Perot etalon and the adjustement of the cavity length. Proper adjustments of the cavity and pump alignments allows to force the laser emission on two adjacent longitudinal modes on orthogonal polarizations, with a frequency difference below the free-spectral range of the cavity.

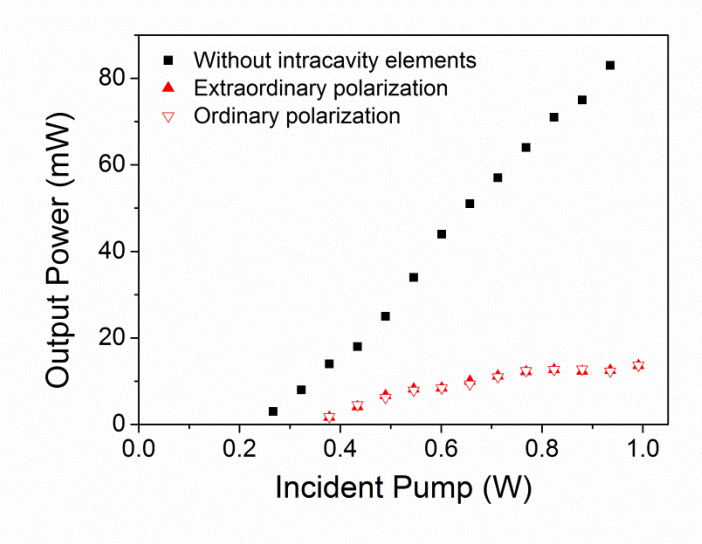

Figure 4: Laser output power versus incident pump power : without any intracavity elements at 855nm (black boxes), and with all the elements in the ordinary and extraordinary polarizations at 852nm (red triangles).

Figure 5 (left) shows the high-resolution optical spectrum of the dual-frequency laser around 852.1 nm, measured with a Fourier Transform optical spectrum analyser, in a configuration for which $\Delta\nu$ is smaller than the FSR of the laser cavity; thus the laser operates on two adjacent cross-polarized modes. The 2-frequency emission is also evidenced in the RF beat-note spectrum obtained by mixing the cross-polarized lines with a polarizer oriented at 45° of their axes and focusing the laser beam onto an ultrafast InGaAs MSM photodetector followed by a RF amplifier (Fig. 5 - right). The frequency difference obtained is around 3 GHz and it can be tuned around ±1GHz changing the MgO:SLT temperature before mode-hopping occurs.

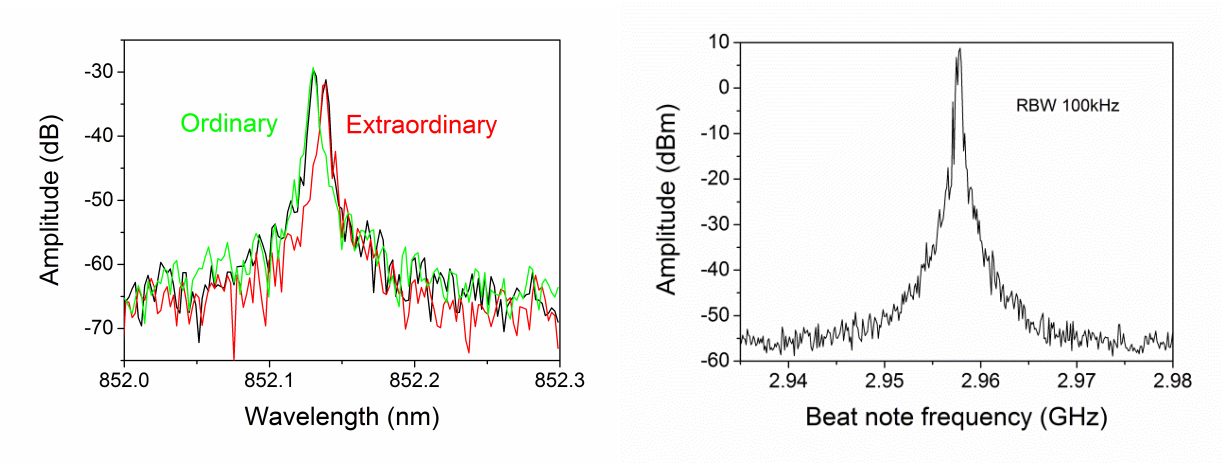

Figure 5 : *Left:* High-resolution optical spectrum of the 2-frequency laser around 852.1nm (resolution = 2 pm). *Right:* Beat note frequency around 3GHz.

4. LASER STABILIZATION

In order for the dual-frequency laser source to be actually used on a Cs-atomic clock, the laser emission has to be stabilized and the noise properties of the laser emission have to be carefully investigated. More precisely, one of the 2 laser lines has to be locked onto a Cs atomic transition line, while the frequency difference is locked at the RF reference at 9.192 GHz. In this section we present the characterization of the frequency stabilization of the dual-frequency laser.
At the output of the laser, the two cross-polarized lines are separated by a polarized beam splitter, and the laser emission is protected from optical feedback with an optical Faraday isolator at each polarization. A small portion (<0.5 mW) of the ordinary-polarized line is injected into a saturated absorption set-up for its stabilization on a Cs atomic transition (see section 4.1). Finally the two lines are recombined and the beatnote is used to lock the frequency difference at a RF reference (see section 4.2). Both servo-loops are tested together to ensure that they are independent and do not influence each other.

4.1 Frequency stabilization at Cs transition

The laser frequency is locked at the top of a Doppler-free transition (F = 4 – F' = 4/5) of the Cs D_2 line using a pump-probe saturated absorption technique, as shown in Figure 6. An acousto-optic crystal is used to modulate the so-called pump beam at 100 kHz to generate the error signal. This method avoids the direct modulation of the pump diode current, which would simultaneously introduce a modulation of the laser intensity; and it provides an error signal with a flat background. Figure 6 right shows the Doppler-free Cs absorption spectrum in a vapor cell from F = 4 hyperfine ground state to the upper levels.

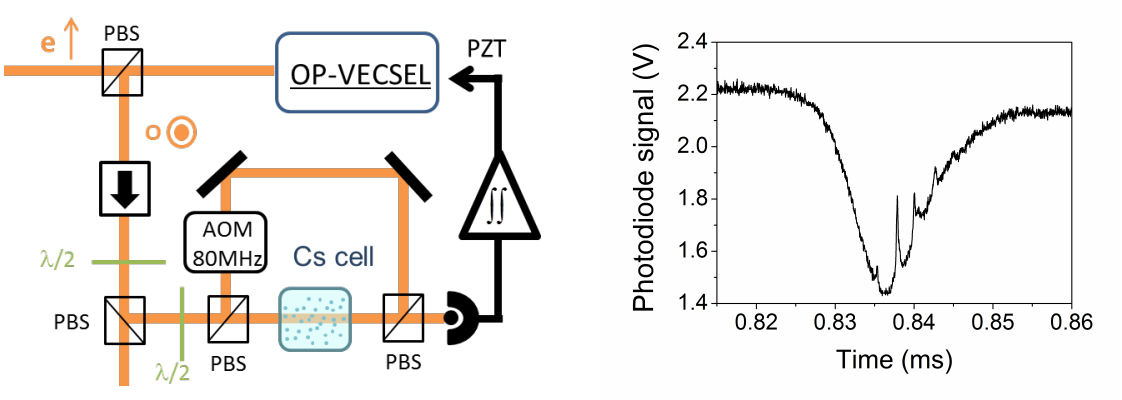

Figure 6: *Left:* Pump-probe satured absorption scheme used to lock the ordinary polarization at the Cs transition. *Right:* Doppler-free Cs absorption spectra.

The error signal is integrated and the correction is made by a low-frequency (1kHz) 2-integration stage servo loop on the piezoelectric transducer glued to the output coupler. The power spectral density of the frequency noise is measured from the error signal with a Fast Fourier Transform analyzer. The servo loop gain reaches 70 dB at low frequencies and its bandwidth is around 600 Hz, limited by the piezoelectric bandwidth (Figure 7).

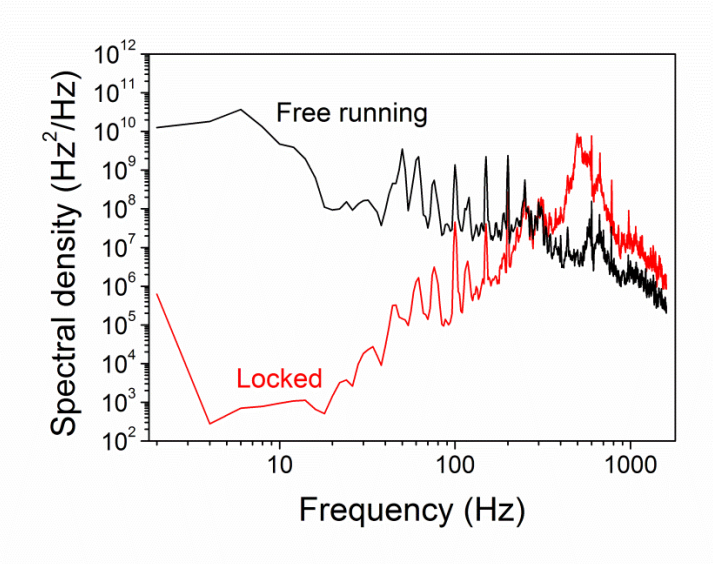

Figure 7 : Spectral density of the error signal of the free running laser and the locked laser at the Cs transition.

4.2 Frequency difference stabilization

The frequency difference between the two laser lines has been locked to a local oscillator (LO) which produces a stable RF reference. The polarization of the ordinary line is rotated with a λ/2 plate and both lines are superimposed on a fast photodiode (bandwidth >12.5GHz). The subsequent beatnote signal is amplified and mixed with the RF reference to generate the error signal, which is amplified with a gain proportional-integral (PI). The low-frequency contribution of the error signal is amplified in a high-voltage amplified, and is recombined with the high-frequency contribution. The error signal is then applied to the electro-optic crystal to compensate for the frequency difference fluctuations. Figure 8 shows a diagram of the set-up.

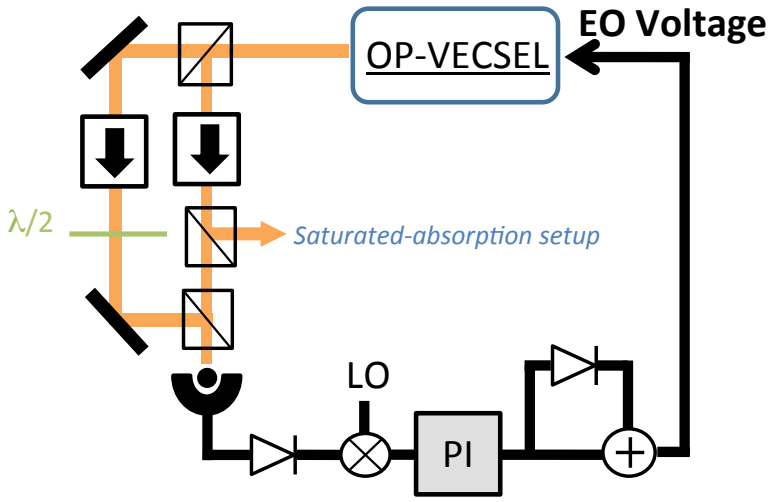

Figure 8 : Experimental set-up of the servo-loop to lock the frequency difference at a RF reference.

Figure 9 shows the beat-note spectra of the free-running laser and of the laser when the frequency difference is locked at the RF reference at 3.2GHz. The servo loop bandwidth is about 1 MHz, it depends on the proportional gain as well as on the electro-optic crystal response. The signal-to-noise ratio is almost 70 dB and the RF beat note linewidth is less than 30Hz, limited by the analyzer resolution (Figure 8 right). Then the two laser lines are strongly phase-locked to each other. The two servo-loops – of the absolute frequency difference on a Cs atomic transition and of the frequency difference on a microwave local oscillator – operate together without perturbing each other.

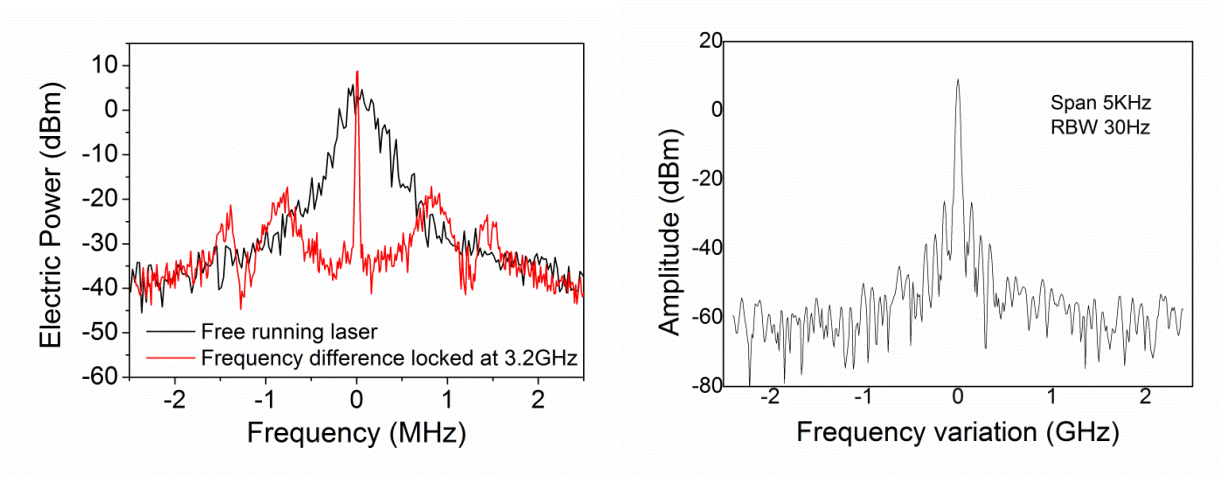

Figure 9: *Left:* Beat note of the free running laser and the frequency difference locked at the RF reference at 3.2GHz. *Right*: Beat note spectrum of the locked laser with a span of 5KHz.

5. CONCLUSION

We have demonstrated the dual-frequency emission of an OP-VECSEL emitting at 852 nm and dedicated to the coherent population trapping of Cs atoms. The laser emission exhibits two narrow lines which are strongly phase-coherent. The laser lines can be precisely tuned, as well as their frequency difference. We have achieved the simultaneous stabilization of both the frequency difference on a local oscillator, and the absolute laser frequency on an atomic transition.

Further characterization of the noise properties (intensity and phase) of the laser source is necessary, but still the optical properties of this dual-frequency laser source are already compatible with requirements for a CPT atomic clock. Dual-

frequency OP-VECSEL emitting at the wavelength of a Cs transition might thus be an innovating solution with major potentials for miniature atomic clocks.

REFERENCES

[1] J. Kitching, S. Knappe, N. Vukicevic, L. Hollberg, R. Wynands, and W. Weidmann, "A Microwave Frequency Reference Based on VCSEL-Driven Dark Line Resonances in Cs Vapor", IEEE Trans. Instr. Meas., vol. 49, no. 6, pp 1313-1317, Dec. 2000

[2] Merimaa, M., Lindvall, T., Tittonen, I. and Ikonen, E., "All-optical atomic clock based on coherent population trapping in 85Rb" J. Opt. Soc. Amer. B, Opt. Phys. 20(2), 273–279 (2003)

[3] Le Gouët, J., Morvan, L., Alouini, M., Bourderionnet, J., Dolfi, D. and Huignard,J.-P, "Dual-frequency single-axis laser using a lead lanthanum zirconate tantalate (PLZT) birefringent etalon for millimeter wave generation: beyond the standard limit of tunability", Opt. Let. 32(9), 1090-1093 (2007)

[4] Czarny, R., Alouini, M., Larat, C., Krakowski, M. and Dolfi D., "THz-dual-frequency Yb3:KGd(WO4)2 laser for continuous wave THz generation through photomixing", Elec. Let. 40(15) 942-943 (2004)

[5] Baili, G., Morvan, L., Alouini, M., Dolfi, D., Bretenaker, F., Sagnes, I. and Garnache, A., "Experimental demonstration of a tunable dual-frequency semiconductor laser free of relaxation oscillations", Opt. Lett. 34, 3421-3423 (2009)

[6] J. E. Hastie, J. M. Hopkins, S. Calvez, C. W. Jeon, D. Burns, R. Abram, E. Riis, A. I. Ferguson, and M. D. Dawson, "0.5-W single transverse-mode operation of an 850-nm diode-pumped surface-emitting semiconductor laser," IEEE Photon. Technol. Lett. 15, 894–896 (2003)

[7] A. Laurain, M. Myara, G. Beaudoin, I. Sagnes, A. Garnache, " Multiwatt–power highly–coherent compact single–frequency tunable Vertical–External–Cavity–Surface– Emitting–Semiconductor–Laser", Optics Express 18, 14, 14627 (2010)

[8] Rösener, B., Kaspar, S., Rattunde, M., Töpper, T., Manz, C., Köhler, K.,Ambacher,O. and Wagner, J. "2µm semiconductor disk laser with a heterodyne linewidth below 10 kHz", Opt. Lett. 36, 3587 (2011)

[9] Cocquelin, B., Lucas-Leclin, · G., Georges, · P., Sagnes, ·I. and Garnache, A. "Design of a low-threshold VECSEL emitting at 852nm for Cesium atomic clocks", Opt Quant Electron 40,167–173 (2008).

[10] Baili, G., Alouini, M., Dolfi, D., Bretenaker, F., Sagnes, I. and Garnache, A., "Shot-noise-limited operation of a monomode high-cavity-finesse semiconductor laser for microwave photonics applications", Opt. Lett. 32, 650 (2007)

[11] A. Garnache, A. A. Kachanov, F. Stoeckel, R. Houdre, " Diode-pumped broadband vertical-external-cavity surface-emitting semiconductor laser applied to high-sensitivity intracavity absorption spectroscopy", JOSA B, vol. 17, 9, 1589 (2000)

[12] V. Pal, P. Trofimoff, B.-X. Miranda, G. Baili, M. Alouini, L. Morvan, D. Dolfi, F. Goldfarb, I. Sagnes, R. Ghosh, and F. Bretenaker "Measurement of the coupling constant in a two-frequency VECSEL", Opt. Exp. 18, 5008 (2010)

[13] Casson, J. L., Gahagan, K. T., Scrymgeour, D. A., Jain, R. K., Robinson, J. M., Gopalan, V., Snader, R. K. "Electro-optic coefficients of lithium tantalite at near-infrared wavelengths", J. Opt. Soc. Am. B 21, 1948 (2004).

[14] Dolev, I., Ganany-Padowicz, A., Gayer, O., Arie, A., Mangin, J and Gadret, G. "Linear and nonlinear optical properties of MgO:$LiTaO_3$", Appl. Phys. B. 96, 423 (2009).